Electronic Supplementary Material (ESI) for New Journal of Chemistry.

Supporting Information for

Comparative Study of the Photophysical and Crystallographical Properties of 4-(9*H*-Pyreno[4,5-*d*]imidazol-10-yl)phenol and Its Alkylated Derivatives

*Zahra A. Tabasi, Joshua C. Walsh, Graham J. Bodwell, David W. Thompson, and Yuming Zhao**

Department of Chemistry, Memorial University, St. John's, Newfoundland and Labrador, CANADA A1B 3X7; yuming@mun.ca

Table of Content

1. Experimental

1.1 Synthesis and Characterization

Compound **1** was prepared using the previously reported synthetic method.[1] Alkylation of **1** resulted in the formation of compounds **2** and **3**, which were separated by silica flash column chromatography. All compounds were subjected to NMR, IR, and MS analyses to confirm their structures and purity. ^{1}H and ^{13}C NMR spectra were measured on a Bruker 300 MHz AVANCE III spectrometer. Infrared (IR) spectra were recorded on a Bruker Alfa spectrometer. High-resolution mass spectrometric (HRMS) analyses were performed on a GCT premier Micromass Technologies instrument.

4-(9*H*-Pyreno[4,5-*d*]imidazol-10-yl)phenol (**1**)

Pyrene-4,5-dione (0.20 g, 0.86 mmol), *p*-hydroxybenzaldehyde (0.32 g, 2.6 mmol), ammonium acetate (1.3 g, 17 mmol), and glacial acetic acid (99.7%, 7 mL) were mixed in a round-bottom flask equipped with a condenser. The reaction was heated at 110 °C for 5 h, and then slowly cooled down to rt. The resulting precipitate was collected by vacuum filtration and then sequentially washed with glacial acetic acid, saturated $NaHCO_3$ solution (aq), and water to yield crude product **1**, which was subjected to silica flash column chromatography using EtOAc/hexanes (10:90, v/v) as eluent to afford pure compound **1** (0.15 g, 0.45 mmol, 52%, R_f = 0.22) as a black solid. IR (neat): 3612, 3458, 3221, 2920, 2852, 1728, 1605, 1541, 1248, 1175, 889, 762, 716 cm^{-1}; ^{1}H NMR (300 MHz, CD_3OD): δ 8.77 (d, J = 7.5 Hz, 2H), 8.18–8.02 (m, 8H), 7.03 (d, J = 8.8 Hz, 2H) ppm; A meaningful ^{13}C NMR spectrum was not obtained due to limited solubility; HRMS (MALDI-TOF): *m/z* calcd for $C_{23}H_{15}N_2O$ $[M + H]^+$ 335.1184 found 335.1171.

10-(4-(Decyloxy)phenyl)-9*H*-pyreno[4,5-*d*]imidazole (**2**)

To a solution of compound **1** (0.10 g, 0.30 mmol) in absolute ethanol (7.0 mL) were added 1-bromodecane (0.066 g, 0.30 mmol) and potassium carbonate (0.041 g, 0.30 mmol). The reaction mixture was heated at reflux for 4 h, and then another portion of potassium carbonate (0.020 g, 0.15 mmol) was added. After keeping reflux for another 6 h, the reaction mixture was slowly cooled down to rt. The solvent was removed by rotary evaporation and the crude mixture of alkylated products was purified by silica flash column chromatography using EtOAc/hexanes (5:95, v/v) as eluent. Compound **2** (0.064 g, 0.13 mmol, 43%, R_f = 0.59) was obtained as a white crystalline solid. IR (neat): 3498, 3359, 2946, 2852, 1632, 1613, 1468, 1248, 1185, 998, 716, 666 cm^{-1}; ^{1}H NMR (300 MHz, acetone-d_6): δ 13.54 (s, 1H, NH), 8.91–8.71 (m, 2H), 8.31 (d, J = 8.9 Hz, 2H), 8.24 (d, J = 6.5 Hz, 2H), 8.22–8.09 (m, 4H), 7.18 (d, J = 8.9 Hz, 2H), 4.09 (t, J = 6.5 Hz, 2H), 1.85–1.66 (m, 2H), 1.52–1.18 (m, 14H), 0.86 (t, J = 6.9 Hz, 3H) ppm; ^{13}C NMR (75

[1] (a) Z. A. Tabasi, E. A. Younes, J. C. Walsh, D. W. Thompson, G. J. Bodwell, Y. Zhao, *ACS Omega* **2018**, *3*, 16387-16397; (b) Z. A. Tabasi, J. C. Walsh, G. J. Bodwell, D. W. Thompson, Y. Zhao, *Cryst. Growth Des.* **2020**, *20*, 1681-1693.

MHz, acetone-d_6): δ 160.2, 150.1, 137.9, 132.1, 131.9, 128.3, 128.2, 127.9, 126.8, 126.6, 123.3, 122.2, 122.0, 119.5, 119.3, 119.2, 115.3, 68.1, 31.8, 29.5, 29.4, 29.3, 29.2, 26.0, 22.6, 14.4 ppm (four aromatic and one aliphatic carbon signals not observed due to coincidental overlap); HRMS (MALDI-TOF): *m/z* calcd for $C_{33}H_{35}N_2O$ $[M + H]^+$ 475.2749 found 475.2752.

9-Decyl-10-(4-(decyloxy)phenyl)-9*H*-pyreno[4,5-*d*]imidazole (**3**)

In the above alkylation reaction, compound **3** (0.046 g, 0.075 mmol, 25%, R_f = 0.76) was obtained as a white crystalline solid after silica column chromatographic separation. IR (neat): 2918, 2848, 1591, 1426, 1242, 1180, 1016, 824, 715, 657, 630, 540 cm^{-1}; ^1H NMR (300 MHz, acetone-d_6): δ 8.96 (dd, *J* = 7.6, 1.3 Hz, 1H), 8.70 (d, *J* = 7.9 Hz, 1H), 8.26–8.22 (m, 2H), 8.21–8.08 (m, 4H), 7.81 (d, *J* = 8.8 Hz, 2H), 7.18 (d, *J* = 8.8 Hz, 2H), 4.88 (t, *J* = 7.5 Hz, 2H), 4.14 (t, *J* = 6.5 Hz, 2H), 1.94–1.78 (m, 2H), 1.60–1.49 (m, 2H), 1.49–11.5 (m, 28H), 0.90 (t, *J* = 7.0 Hz, 3H), 0.84 (t, *J* = 6.9 Hz, 3H) ppm; ^{13}C NMR (75 MHz, acetone-d_6): δ 160.2, 153.2, 138.5, 132.4, 131.8, 131.4, 127.8, 127.7, 126.9, 126.2, 126.0, 124.1, 124.0, 123.6, 123.0, 119.3, 118.2, 114.5, 67.9, 46.6, 31.75, 31.68, 29.2, 29.0, 25.93, 25.86, 22.44, 22.38, 13.5, 13.4 ppm (three aromatic carbon signals not observed due to coincidental overlap, and eight aliphatic carbon signals not observed due to overlap with solvent signals); HRMS (MALDI-TOF): *m/z* calcd for $C_{43}H_{55}N_2O$ $[M + H]^+$ 615.4314 found 615.4290.

1.2 UV-Vis absorption and fluorescence spectroscopic analysis

UV–Vis absorption spectra were recorded using a Cary 6000i spectrophotometer. Fluorescence spectra were measured on a Photon Technology International (PTI) QuantaMaster spectrofluorometer. Relative fluorescence quantum yields (ϕ_F) were measured following reported procedures using quinine sulfate (ϕ_F = 0.546) as the standard.[2]

1.3 Crystallization conditions and X-ray crystallographic analysis

Single crystals of compounds **1**–**3** suitable for X-ray diffraction analysis were grown from mixture of solvents (1:1 hexanes/methanol for 1, and 5:95 ethyl acetate/hexanes for **2** and **3**) by slow evaporation at room temperature. Single-crystal X-ray diffraction (SXRD) analysis was performed on a Bruker PLATFORM/APEX II CCD diffractometer, and the crystal structures were solved by direct methods using the *SHELXD* program[3] and refined by full-matrix least-squares methods with *SHELXL–2014*.[4] Hirschfeld surface analysis was carried out using the *CrystalExplore* software package.[5]

[2] A. T. R. Williams, S. A. Winfield, J. N. Miller, *Analyst* **1983**, *108*, 1067-1071.
[3] T. R. Schneider, G. M. Sheldrick, *Acta Crystallogr. D* **2002**, *58*, 1772-1779.
[4] G. M. Sheldrick, *Acta Crystallogr. C* **2015**, *71*, 3-8.
[5] *CrystalExplorer* (Version 3.1), S. K. Wolff, D. J. Grimwood, J. J. McKinnon, M. J. Turner, D. Jayatilaka, M. A. Spackman, University of Western Australia, 2012.

2. NMR Spectra of Compounds 1-3

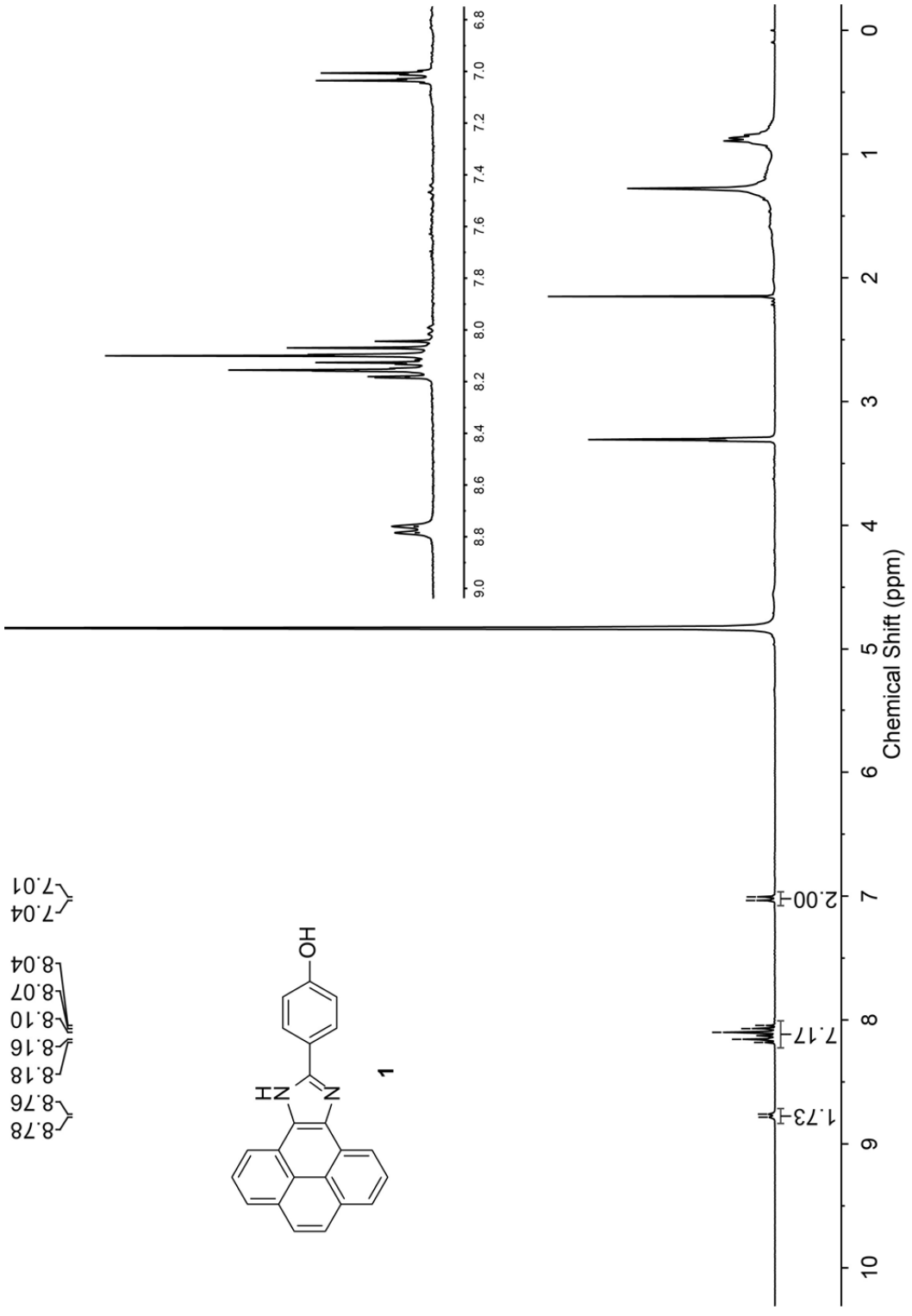

Fig. S-1 ^{1}H NMR (300 MHz, CD_3OD) spectrum of compound **1**.

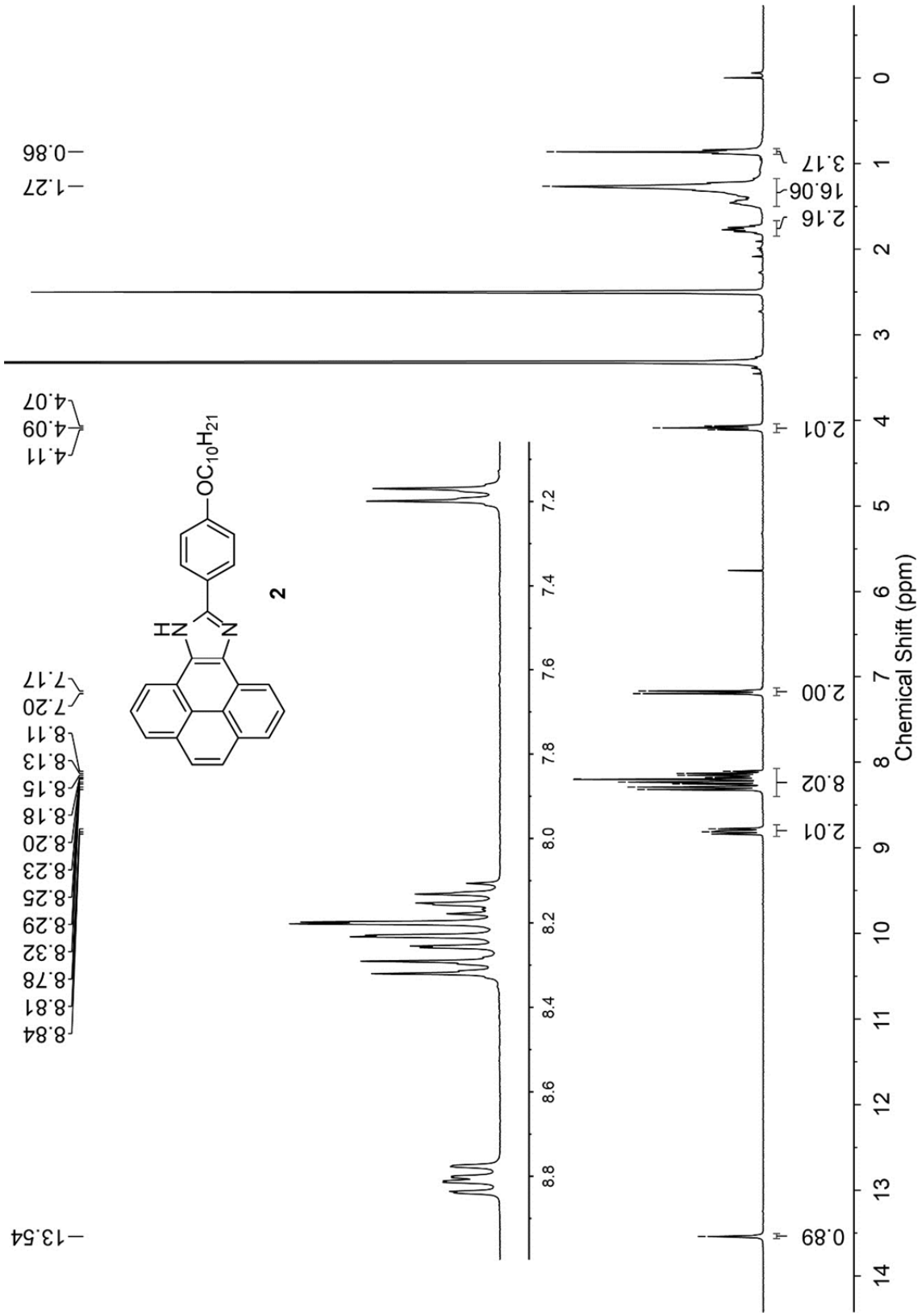

Fig. S-2 ^{1}H NMR (300 MHz, acetone-d_6) spectrum of compound **2**.

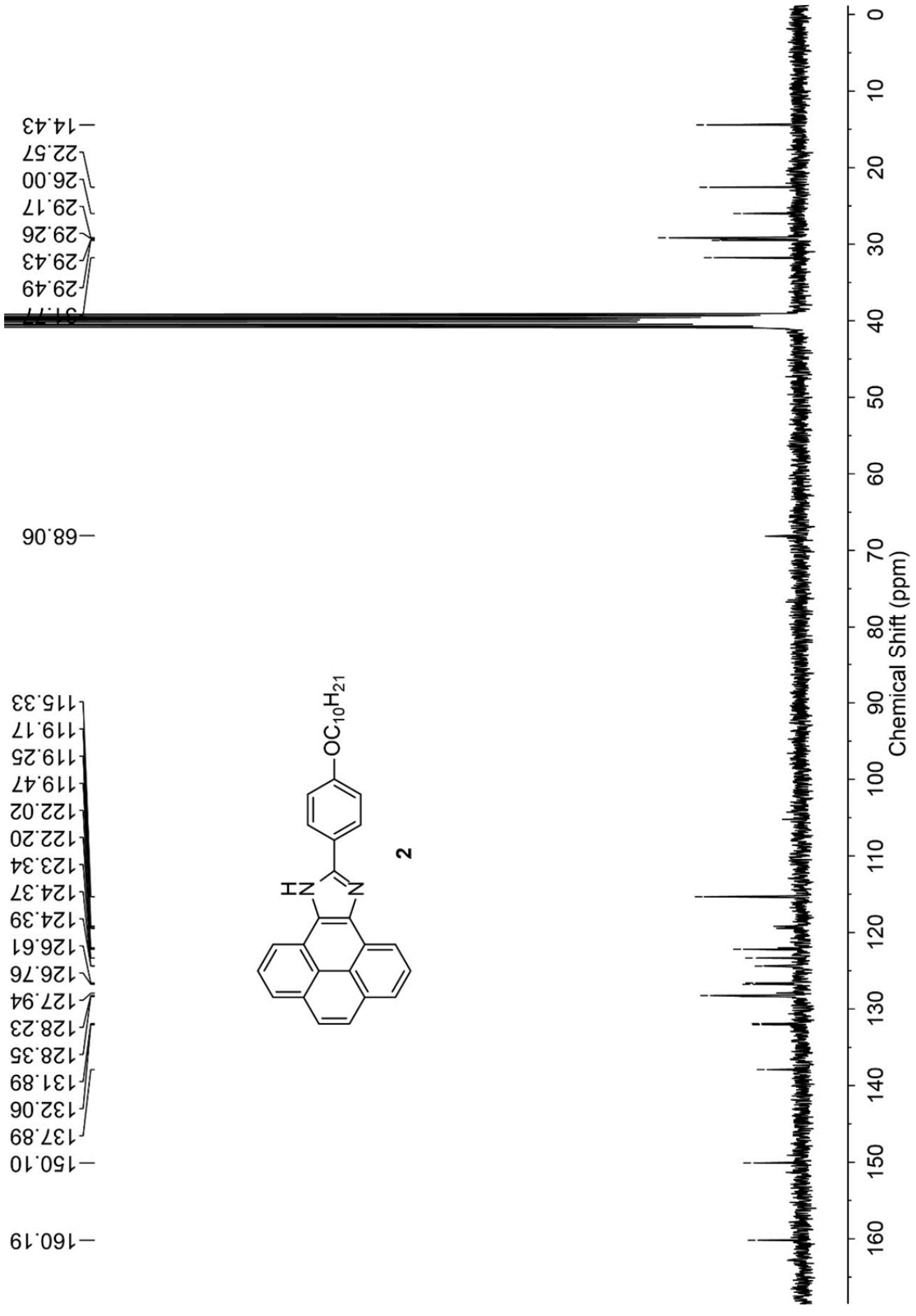

Fig. S-3 ^{13}C NMR (75 MHz, acetone-d_6) spectrum of compound **2**.

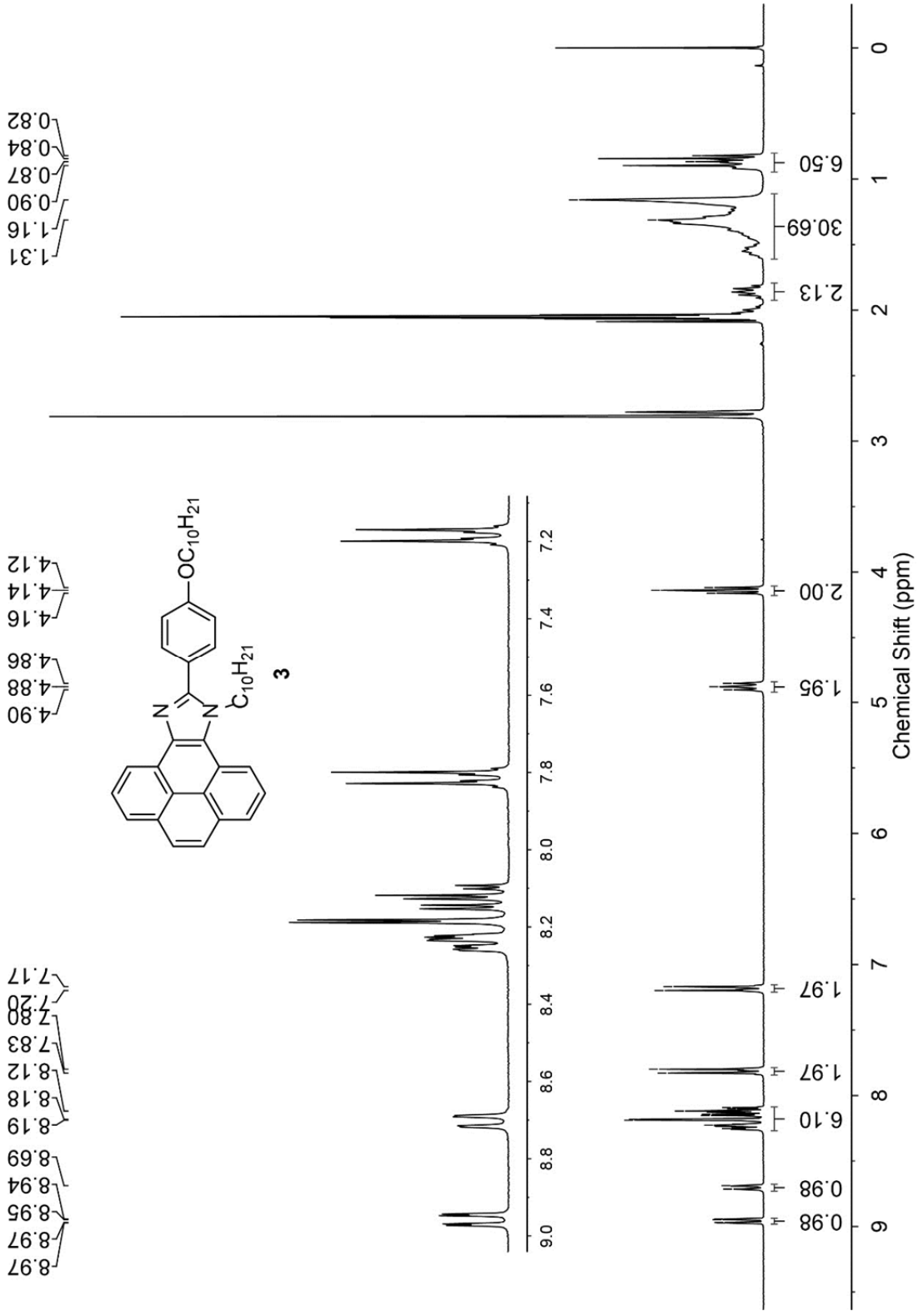

Fig. S-4 ^{1}H NMR (300 MHz, acetone-d_6) spectrum of compound **3**.

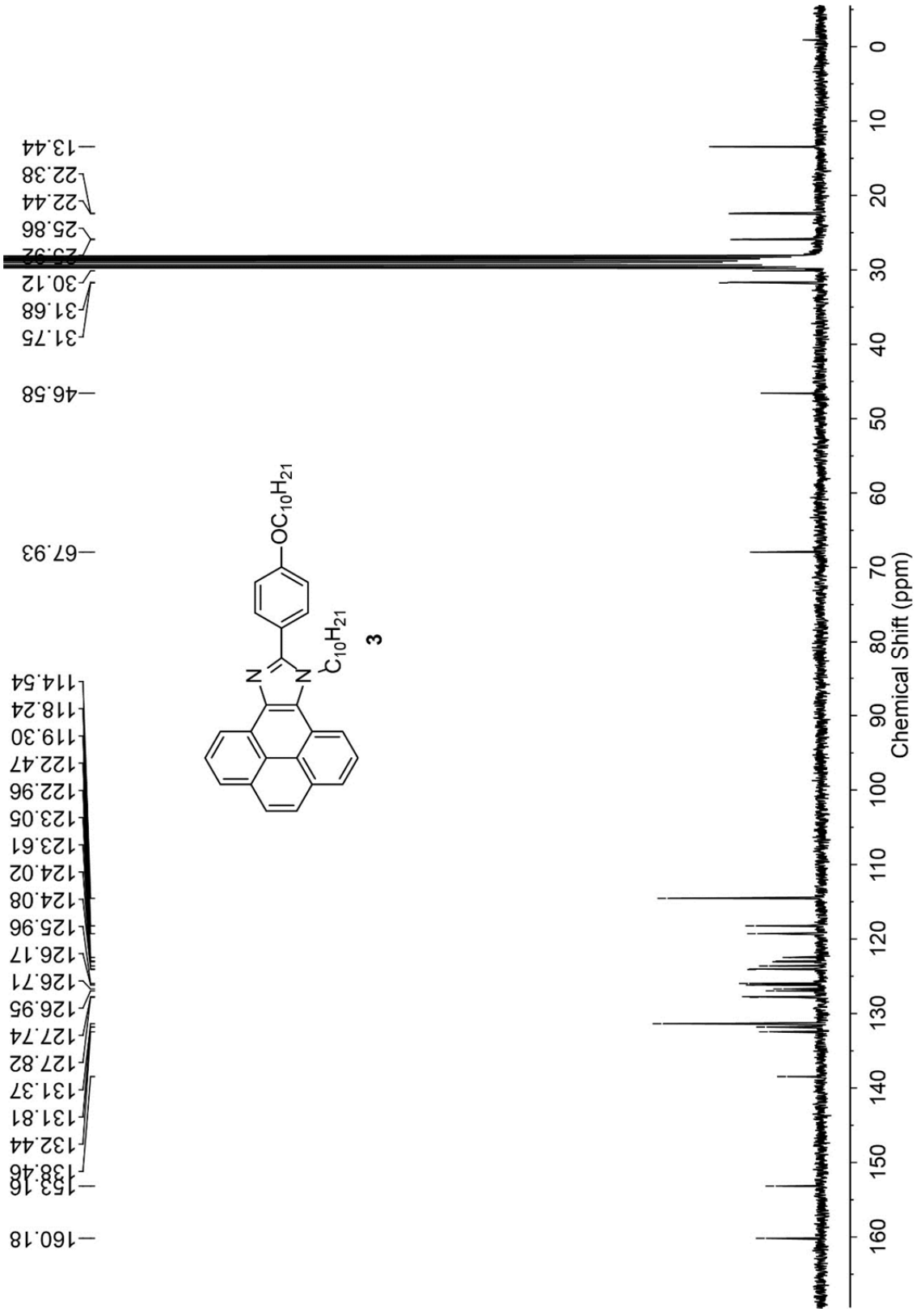

Fig. S-5 ^{13}C NMR (75 MHz, acetone-d_6) spectrum of compound **3**.

2. Crystallographic Data for Compounds 1-3

Table S-1 Crystallographic and experimental data for compound **1**

Empirical formula	$C_{24}H_{18}N_2O_2$
Formula weight	366.40
Temperature/K	-173
Crystal system	monoclinic
Space group	$P2_1/n$ (an alternate setting of $P2_1/c$ [No. 14])
a/Å	12.6038(2)
b/Å	8.2717(2)
c/Å	18.3638(4)
β/°	109.1087(12)
Volume/Å^3	1809.02(7)
Z	4
ρ_{calc} g/cm^3	1.345
μ/mm^{-1}	0.691
Crystal size/mm^3	0.14 × 0.13 × 0.10
Radiation	Cu K_α (1.54178) (microfocus source)
2Θ range for data collection/°	7.50 to 147.70
Index ranges	$-15 \le h \le 15$, $-10 \le k \le 10$, $-22 \le l \le 22$
Reflections collected	12501
Independent reflections	3591 [R_{int} = 0.0212]
Data/restraints/parameters	3591/0/266
Goodness-of-fit (*S*) [all data]	1.079
Final R_1 [$F_o^2 \ge 2\sigma(F_o^2)$]	0.0425
Final wR_2 [all data]	0.1314
Largest diff. peak/hole / e Å^{-3}	0.285/-0.325

Table S-2 Crystallographic and experimental data for compound **2**

Empirical formula	$C_{33}H_{38}N_2O_3$
Formula weight	510.65
Temperature/K	100(2)
Crystal system	triclinic
Space group	*P*-1
a/Å	8.9659(3)
b/Å	8.9998(3)
c/Å	19.2836(7)
α/°	87.414(3)
β/°	79.965(3)
γ/°	63.475(3)
Volume/Å^3	1369.99(9)

Z	2
ρ_{calc} g/cm3	1.238
μ/mm^{-1}	0.620
F(000)	548.0
Crystal size/mm^3	0.15 × 0.1 × 0.05
Radiation	Cu K_α (λ = 1.54184)
2Θ range for data collection/°	4.656 to 155.11
Index ranges	-11 ≤ h ≤ 10, -11 ≤ k ≤ 11, -18 ≤ l ≤ 24
Reflections collected	19003
Independent reflections	5677 [R_{int} = 0.0325, R_{sigma} = 0.0229]
Data/restraints/parameters	5677/0/364
Goodness-of-fit on *F*2	1.058
Final *R* indexes [*I*>=2σ(*I*)]	R_1 = 0.0479, wR_2 = 0.1304
Final *R* indexes [all data]	R_1 = 0.0550, wR_2 = 0.1371
Largest diff. peak/hole / e Å^{-3}	0.28/-0.30

Table S-3 Crystallographic and experimental data for compound **3**

Empirical formula	$C_{43}H_{54}N_2O$
Formula weight	614.88
Temperature/K	-173
Crystal system	triclinic
Space group	$P\bar{1}$ (No. 2)]
a/Å	9.4376(3)
b/Å	11.2292(4)
c/Å	17.0583(6)
α/°	90.117(2)
β/°	93.940(2)
γ/°	101.967(2)
Volume/Å^3	1764.07(11)
Z	2
ρ_{calc} g/cm^3	1.158
μ/mm^{-1}	0.516
Crystal size/mm^3	0.63 × 0.09 × 0.07
Radiation	Cu K_α (λ = 1.54178) (microfocus source)
2Θ range for data collection/°	5.20 to 147.82
Index ranges	-11 ≤ h ≤ 11, -13 ≤ k ≤ 14, -21 ≤ l ≤ 21
Reflections collected	60985
Independent reflections	6879 (R_{int} = 0.0843)
Data/restraints/parameters	6879/0 /417
Goodness-of-fit (*S*) [all data]	1.017
Final R_1 [$F_o^2 \geq 2\sigma(F_o^2)$]	0.0555
Final wR_2 [all data]	0.1633
Largest diff. peak/hole / e Å^{-3}	0.210/-0.331

3. Summary of UV-Vis Absorption Properties for 1-3

Table S-4 Summary of maximum absorption wavelengths (λ_{max}) and corresponding extinction coefficients (ε) for compounds **1-3** in different solvents

Solvent	**1**		**2**		**3**	
	λ_{max} (nm)	ε (mol^{-1} L cm^{-1})	λ_{max} (nm)	ε (mol^{-1} L cm^{-1})	λ_{max} (nm)	ε (mol^{-1} L cm^{-1})
acetone	384	1.41×10^4	384	2.22×10^4	380	1.27×10^4
	364	1.85×10^4	364	2.71×10^4	362 (sh)	2.64×10^4
	349	1.81×10^4	350	2.55×10^4	354	3.18×10^4
					347	3.18×10^4
DMSO	386	1.79×10^4	386	2.55×10^4	381	1.36×10^4
	366	2.01×10^4	366	2.71×10^4	362 (sh)	2.83×10^4
	351	1.71×10^4	352	2.37×10^4	353	3.20×10^4
CH_3CN	383	1.47×10^4	382	2.17×10^4	380	1.29×10^4
	363	1.98×10^4	364	2.71×10^4	361	2.52×10^4
	349	2.00×10^4	349	2.58×10^4	352	3.16×10^4
					347	3.18×10^4
EtOH	382	1.52×10^4	382	2.15×10^4	378	0.98×10^4
	363	1.96×10^4	363	2.60×10^4	359 (sh)	1.95×10^4
	348	2.01×10^4	348	2.72×10^4	349	3.15×10^4
CH_2Cl_2	383	1.14×10^4	384	2.05×10^4	380	1.16×10^4
	363	1.70×10^4	364	2.70×10^4	362 (sh)	2.73×10^4
	348	2.01×10^4	350	2.66×10^4	354	3.17×10^4
toluene	384	0.99×10^4	385	2.11×10^4	382	1.24×10^4
	365 (sh)	1.48×10^4	365	2.71×10^4	363	2.98×10^4
	350	1.92×10^4	352	2.55×10^4	356	3.18×10^4
					348	3.12×10^4

4. NMR Analysis on Solvent Effects

The solvent effects on **Ph-PyIm 1** were investigated by ^{1}H NMR analysis.

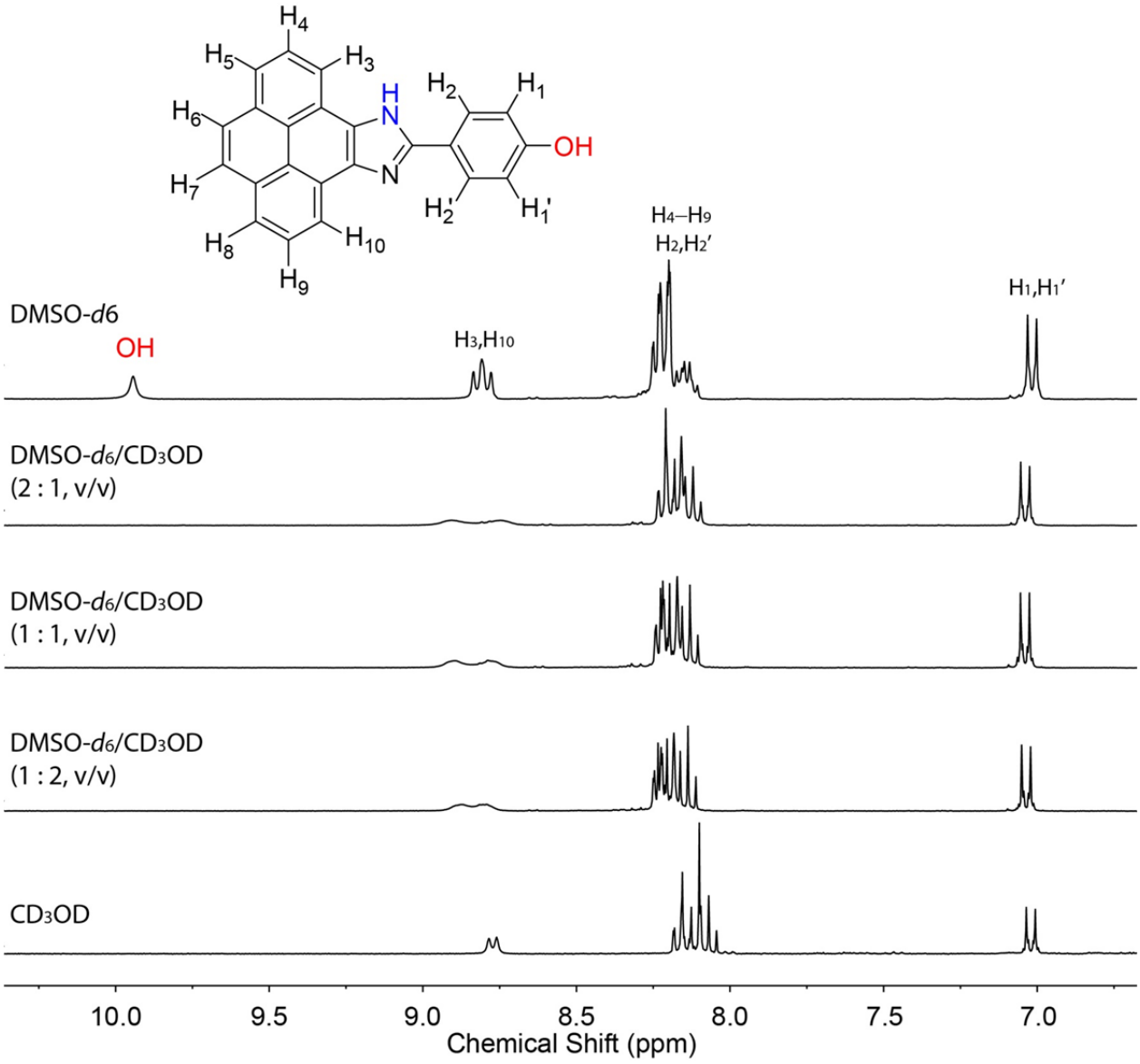

Fig. S-6 Expanded ^{1}H NMR (300 MHz) spectra showing the aromatic region of compound **1** measured in different solvents.

Measured in DMSO-d_6, the imidazolyl NH and phenolic OH protons of **1** are observed at 13.48 ppm and 9.94 ppm in the spectrum. The two phenyl protons *ortho* to the OH group (labeled as H_1/H_1') appear as a pseudo doublet at 7.01 ppm, while phenyl protons H_2/H_2' and

pyrenyl protons H_4–H_9 are overlapped in the region of 8.30–8.09 ppm. The two pyrenyl protons H_3 and H_{10} give rise to a signal at 8.81 ppm, which looks like a "triplet". This signal can be explained as two partially overlapped pseudo doublets, considering the significant splitting effects of H_3 and H_{10} mainly come from the coupling of H_4 and H_9, respectively. This NMR pattern concurs with the solvation motif **A** shown in Scheme S-1. In this solvated structure, proton H_3 should be slightly more shielded than proton H_{10}, due to the hydrogen bonding interaction with DMSO oxygen atom.

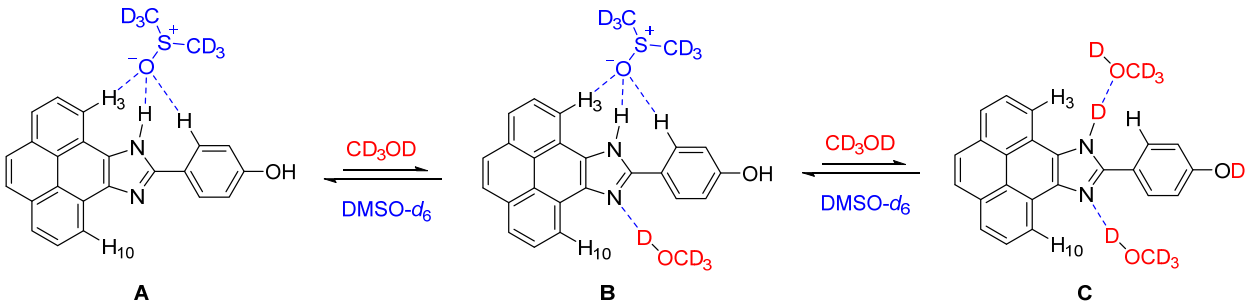

Scheme S-1 Proposed solvent exchange steps for compound **1** in DMSO-d_6 and CD_3OD.

Measured in mixtures of DMSO-d_6 and CD_3OD, the imidazolyl NH and phenolic OH signals disappear completely as a result of rapid proton/deuterium exchanges with CD_3OD. In the meantime, the imidazolyl C=N can form a hydrogen bond with CD_3OD (structure **B** in Scheme S-1). The equilibrium between **A** and **B** results in the signals of H_3 and H_{10} being broad and slightly shifted apart (see the spectrum measured in 2:1 DMSO-d_6 / CD_3OD). As the amount of CD_3OD increases, the line shapes of the two signals for H_3 and H_{10} become narrower and they gradually come closer. Eventually, the H_3 and H_{10} signals merge into a doublet at 8.77 ppm in CD_3OD.

The NMR changes in Figure S-6 reflect different solvation stages as outlined in Scheme S-1. In DMSO-d_6, the solvent molecule interacts with **1** via hydrogen bonds illustrated in structure **A**. In the mixtures of DMSO-d_6 and CD_3OD, the two different solvent molecules compete with one another in hydrogen bonding interactions with **1**, resulting in equilibration among the three structures **A**–**C**. In CD_3OD, the solvent molecules form hydrogen bonds around the imidazolyl unit of **1** (structure **C** in Scheme S-1), and tautomerization of the imidazolyl group makes the two proton signals (H_3 and H_{10}) degenerated.

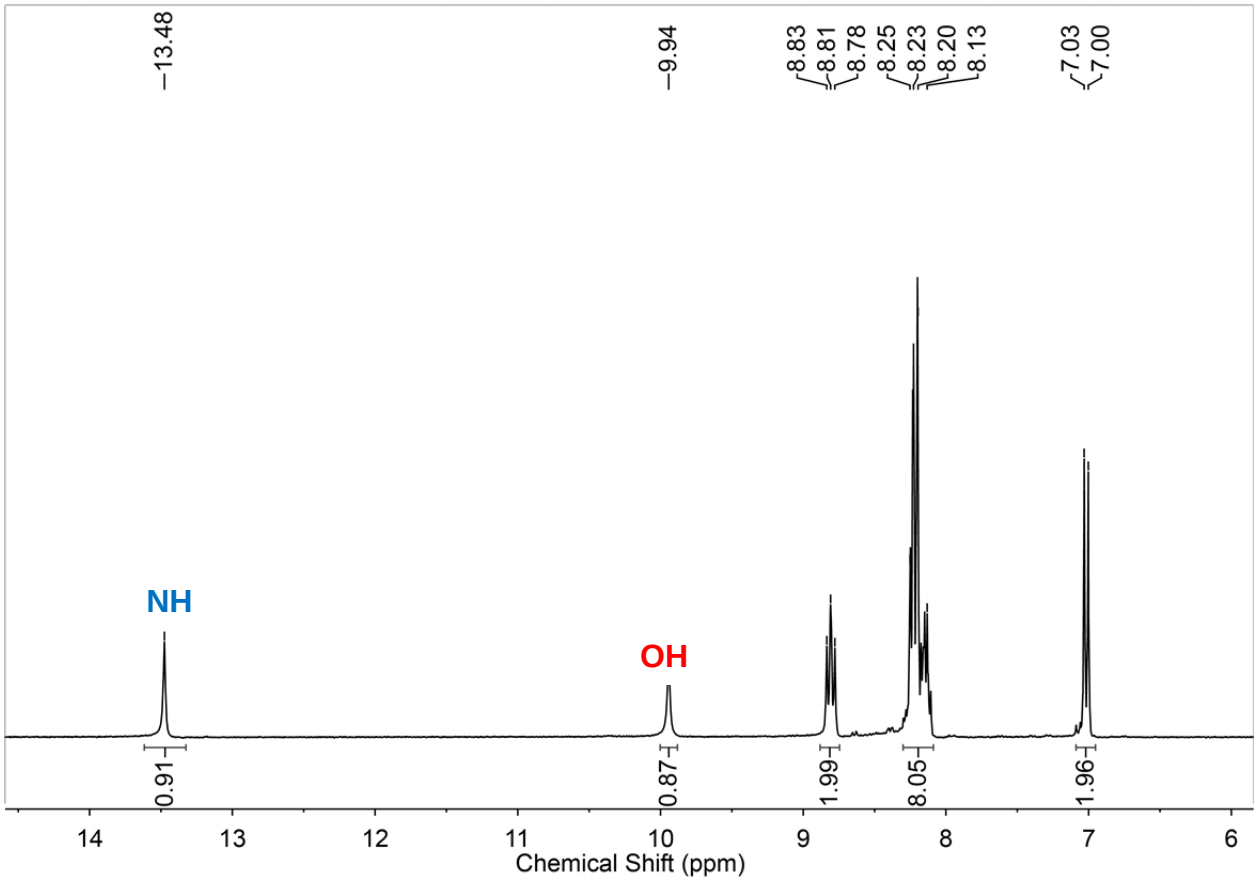

Fig. S-7 Expanded ^{1}H NMR (300 MHz) spectrum showing the aromatic region of compound **1** measured in DMSO-d_6.